Published in The European Physical Journal D - Atomic, Molecular, Optical and Plasma Physics 66, issue 3, 1-14, 2012
which should be used for any reference to this work

Theoretical analysis of aliasing noises in cold atom Mach-Zehnder interferometers

A. Joyet[a], G. Di Domenico, and P. Thomann

Laboratoire Temps-Fréquence (LTF), Université de Neuchâtel, 2000 Neuchâtel, Switzerland

Abstract. We present a theoretical analysis of aliasing noises that might appear in cold atom Mach-Zehnder interferometers used for the measurement of various physical quantities. We focus more specifically on single cold atom gyroscopes. To evaluate the level of aliasing noises, we have developed a model based on the power spectral densities of the different identified noise sources as input parameters and which makes use of a servo-loop to realize a precise measurement of the rotation rate. The model allows one to take into account different modes of operation, like a continuous as well as a pulsed or even a multi-ball operation. For monokinetic atoms, we show that the intermodulation noise can be completely filtered out with a continuous mode of operation and an optimum modulation scheme for any modulation frequency but also with a pulsed operation however only for specific launching frequencies. In the case of a real continuous atomic beam having a velocity distribution, it comes out that a high attenuation can be reached which indicates clearly the potential stability improvement that can be expected from a continuous operation.

1 Introduction

Cold atom interferometers are highly sensitive instruments that can be used to measure very precisely various physical quantities related to inertial motion [1]. Examples of such instruments developed nowadays in several laboratories are gyroscopes [2–5] for the measurement of rotation rates and gravimeters [6,7] for the measurement of the local acceleration of gravity g. Although based on different atoms and geometries, they rely on the same principle of operation which is very close to that of a cold atom fountain clock [8,9] if we replace the microwave Ramsey interrogation by a three-pulse Mach-Zehnder interrogation.

Due to their pulsed mode of operation, they may well suffer from a degradation of their sensitivity similar to the frequency stability degradation appearing in pulsed fountain clocks. Indeed, it is well known that the frequency stability of passive frequency standards operated in pulsed mode, like cold atom fountains, is limited by the phase noise of the oscillator generating the interrogation frequency even with state-of-the-art quartz oscillators [10]. This effect is due to the presence of dead-times in the interrogation and is known as the Dick effect [11,12]. It can only be overcome by the use of very low noise oscillators like cryogenic sapphire oscillators [13].

The present mode of operation of cold atom interferometers is very close to that of a pulsed fountain clock. In this paper, we focus more specifically on Mach-Zehnder gyroscopes. In order to estimate the level of aliasing noises that might appear in such interferometers and potentially limit their sensitivity, we have developed a model that uses the power spectral densities of the different noise sources as input parameters and makes use of a servo-loop to achieve the measurement of the rotation rate. We compute the power spectral density of the rotation rate in closed loop operation and finally the corresponding Allan variance. The model should also make it possible the study and comparison of interferometers's performances for a continuous and a pulsed, or even a multi-ball, mode of operation.

We first describe, in Section 2, the main components of the model for a gyroscope operated in a continuous way. Then, the power spectral density of the fluctuations of the local oscillator frequency used to control the interference fringes is derived in detail in Section 3. In Section 4, the Allan variance of the rotation rate is obtained which is the basic result of our model. Finally in Section 5, we present a discussion of the result obtained in Section 4 for different conditions of operation of the gyroscope.

2 Description of the model

2.1 Idealized Mach-Zehnder interferometer

As a starting point, we consider the case of an idealized spatial-domain and continuous gyroscope, sketched in Figure 1, which satisfy the following simplifying hypothesis. There is one atom source that creates a continuous monokinetic beam of slow and cold atoms in the state

[a] e-mail: alain.joyet@unine.ch

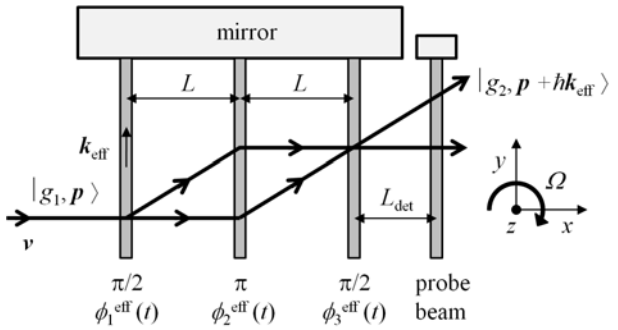

Fig. 1. Sketch of a cold atom Mach-Zehnder interferometer used for the measurement of rotations. We assumes that the three Raman laser beams are in the horizontal plane and retroreflected by one large mirror. L is the distance between two Raman laser beams and L_{det} is the distance of the probe beam from the last Raman beam. $\boldsymbol{k}_{\text{eff}}$ is the effective wave vector of the Raman beams.

$|g\rangle = |g_1, \boldsymbol{p}\rangle$ where the atoms are in the lower hyperfine level of the ground state g_1 with a momentum $\boldsymbol{p}$. The atoms follow an open parabolic trajectory with a horizontal velocity component v and cross three horizontal Raman laser beams perpendicular to $\boldsymbol{p}$. The three Raman beams are retroreflected by one large mirror and spatially separated by a distance L.

To keep the model as simple as possible, we do not take into account the dynamics of the Raman interactions [14]. The transverse dimension of the laser beams is thus supposed to be negligible and the power is adjusted in order to generate, during the crossing by the atoms, three infinitesimally-short Raman pulses $\pi/2 - \pi - \pi/2$ corresponding to a Mach-Zehnder type interferometer. However, we know that the finite duration of the Raman pulses introduces a low-pass filtering of the noise components of the Raman phase. Therefore, to keep a physical meaning to this idealized modelization of the beam splitters, we will include in the transfer function of the interferometer an equivalent low-pass filter that simulates a finite interaction time.

At the output of the interferometer, the atoms are detected in the excited state $|e\rangle = |g_2, \boldsymbol{p} + \hbar\boldsymbol{k}_{\text{eff}}\rangle$ where the atoms are in the higher hyperfine level of the ground state g_2 with a momentum $\boldsymbol{p} + \hbar\boldsymbol{k}_{\text{eff}}$. The effective wave vector of the Raman beams $\boldsymbol{k}_{\text{eff}} = \boldsymbol{k}_{\text{L1}} - \boldsymbol{k}_{\text{L2}}$ is assumed to be identical for all the three beams, where $\boldsymbol{k}_{\text{L1}}$ and $\boldsymbol{k}_{\text{L2}}$ are the wave vectors of the laser beams L1 and L2 respectively, which are superimposed in each Raman interaction (cf. Fig. 3). The frequency ω_0 of the Raman transition corresponds to $\omega_0 = \hbar^{-1}(E_{g_2} - E_{g_1})$ where E_{g_1} and E_{g_2} are the energy levels of the ground state g_1 and g_2 respectively. For the atoms usually used in such interferometers, this frequency ranges in the microwave domain.

Within theses approximations, the time-dependent probability $P_e(t)$ to find the atoms in the excited state $|e\rangle$ at the output of the interferometer is given by the simple expression

$$P_e(t) = \frac{1}{2}\left\{1 - C\cos\left(\Phi(t)\right)\right\} \tag{1}$$

where C represents the contrast of the interference fringes and $\Phi(t)$ is the instantaneous apparent phase of the interferometer. This total phase results from the effect of the laser fields and of the inertial forces acting on the atoms. It can be written as a sum of three terms

$$\Phi(t) = \Phi_{\text{rot}}(t) + \Phi_{\text{acc}}(t) + \Phi_{\text{L}}(t). \tag{2}$$

The first term $\phi_{\text{rot}}(t)$ corresponds to the inertial atomic phase due to a rotation $\boldsymbol{\Omega}(t)$ of the interferometer. We suppose that the rotation rate $\Omega(t)$ varies very slowly with respect to the atomic motion, i.e. $\dot{\Omega}(t)\,T \ll \Omega(t)$ where $T = Lv^{-1}$ is the atom transit time between two successive Raman beams and the dot stands for time derivative. If, moreover, we suppose that there are no fluctuations of the effective wave vector $\boldsymbol{k}_{\text{eff}}$, the atom's velocity $\boldsymbol{v}$ and the distance L, the phase $\Phi_{\text{rot}}(t)$ can be written, at a first order, by

$$\Phi_{\text{rot}}(t) = +\,2\,\frac{L^2}{v^2}\,\boldsymbol{k}_{\text{eff}} \cdot (\boldsymbol{\Omega}(t) \times \boldsymbol{v})\,. \tag{3}$$

The second term $\Phi_{\text{acc}}(t)$ represents the component of the inertial atomic phase due to a net, slowly varying, acceleration $\boldsymbol{a}(t)$ of the interferometer. Within the same approximations, $\dot{a}(t)\,T \ll a(t)$, it is given by

$$\Phi_{\text{acc}}(t) = -\,\frac{L^2}{v^2}\,\boldsymbol{k}_{\text{eff}} \cdot \boldsymbol{a}(t). \tag{4}$$

In this paper, we will focus on the use of a Mach-Zehnder interferometer as a gyroscope. Therefore, we admit that the interferometer is not subjected to any net acceleration and that the phase $\Phi_{\text{acc}}(t)$ is always equal to zero.

The last term $\Phi_{\text{L}}(t)$ is the instantaneous global phase imprinted by the laser fields on the atoms at the end of the Mach-Zehnder interrogation. It can be expressed from the instantaneous individual effective phases $\phi_1^{\text{eff}}(t)$, $\phi_2^{\text{eff}}(t)$ and $\phi_3^{\text{eff}}(t)$ imprinted on the atoms during each Raman interaction by the well known relation

$$\begin{aligned}\Phi_{\text{L}}(t) = {} & \phi_1^{\text{eff}}(t - 2T - T_{\text{det}}) - 2\,\phi_2^{\text{eff}}(t - T - T_{\text{det}}) \\ & + \phi_3^{\text{eff}}(t - T_{\text{det}})\end{aligned} \tag{5}$$

where $T_{\text{det}} = L_{\text{det}}v^{-1}$ is the detection time of flight between the last Raman beam and the probe beam. Each individual effective phase $\phi_i^{\text{eff}}(t)$ for $i = 1, 2$ and 3 is the difference $\phi_i^{\text{eff}}(t) = \phi_{\text{L1},i}(t) - \phi_{\text{L2},i}(t)$ of respectively the phases $\phi_{\text{L1},i}(t)$ and $\phi_{\text{L2},i}(t)$ of the first (L1) and second (L2) laser beam, taken at the position of the atomic wave packet center, which are superimposed in the ith Raman interaction (cf. Fig. 3).

2.2 Principle of the servo-loop

A means to accurately measure the rotation rate $\Omega(t)$ of the gyroscope is to keep permanently the central fringe of the interference pattern at the same position by compensating for the inertial phase shift $\Phi_{\text{rot}}(t)$, due to rotation, by a phase $\Phi_{\text{c}}(t)$ controlled by a servo-loop. In closed loop

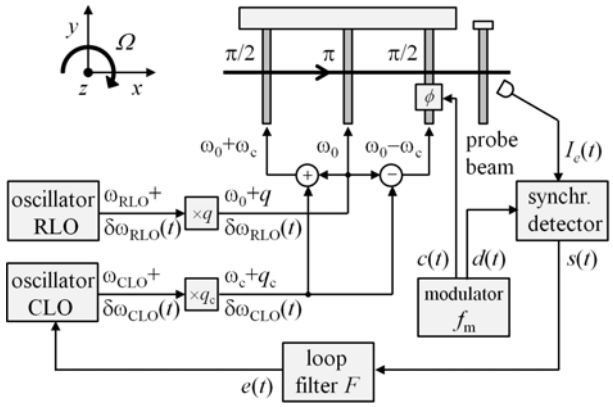

Fig. 2. Block-diagram of the servo-loop considered for the measurement of the gyroscope's rotation rate. The Raman frequency ω_0 and the compensation frequency ω_c are generated from the Raman local oscillator (RLO) and from the compensation local oscillator (CLO). The Raman frequency ω_0 lies in the microwave domain and the compensation frequency ω_c is of the order of 10 Hz.

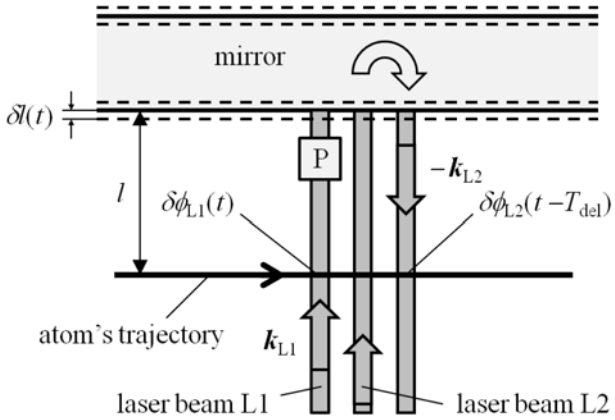

Fig. 3. Sketch of the beam splitter of each three Raman interactions. In the velocity-sensitive configuration, only the laser beam L2 is retroreflected while the retroreflection of the laser beam L1 is blocked with a polarizer (P). The two beams L1 and L2 are to be understood as being superimposed actually.

operation, the phase $\Phi_c(t)$ will be exactely equal to the inertial phase shift $\Phi_{rot}(t)$ thus permitting a precise measurement of $\Phi_{rot}(t)$, i.e. of $\Omega(t)$, by the measurement of $\Phi_c(t)$ through the frequency used as the input parameter of the servo-loop. In doing so, we replace the measurement of the rotation rate $\Omega(t)$ by the measurement of a frequency delivered by an oscillator which can be achieved with high accuracy.

The block-diagram of the servo-loop considered for the measurement of the gyroscope's rotation rate is shown in Figure 2. The phase $\Phi_c(t)$ is generated by applying a frequency offset $+\omega_c(t)$ on the Raman frequency ω_0 in the first $\pi/2$ pulse and a second one $-\omega_c(t)$ in the last $\pi/2$ pulse. In fact, this is equivalent to simulate a rotation of the gyroscope opposed to that of the Earth and thereby cancelling it. This way of doing has the advantage of being symmetrical with respect to a velocity reversal of the atoms which could be useful in the case of a dual gyroscope.

The corresponding instantaneous individual effective phases due to the frequency offset can then be written for the first ($i = 1$) and the third ($i = 3$) Raman pulses

$$\phi_{i,c}^{\text{eff}}(t) = \int_{t_0}^{t} \omega_c(t')\,dt' \tag{6}$$

where t_0 defines the time origin of the application of the frequency offset $\omega_c(t)$. It is composed of a constant value ω_c and a random component

$$\omega_c(t) = \omega_c + q_c\delta\omega_{CLO}(t) \tag{7}$$

with $\delta\omega_{CLO}(t)$ representing the instantaneous angular frequency fluctuations of the free runing compensation local oscillator (CLO) used to generate $\omega_c(t)$ and q_c is the multiplying factor of the CLO frequency ω_{CLO}. Putting (6) and (7) into (5), we get a constant phase which is independent of t_0

$$\Phi_{L,c} = -2\,\omega_c T \tag{8}$$

for the global phase due to the frequency offset and a random part

$$\delta\Phi_{L,c}(t) = -q_c \int_{t-2T-T_{det}}^{t-T_{det}} \delta\omega_{CLO}(t')\,dt'. \tag{9}$$

To get the error signal used by the servo-loop to adjust the frequency $\omega_c(t)$, we modulate the phase of the last Raman pulse at a modulation frequency f_m. This should be of advantage for a real gyroscope with a non-monokinetic atomic beam as discussed in Section 5.4. If this phase modulation is applied on the laser beam L1 for example, the corresponding individual effective phase of the last Raman beam reads

$$\phi_{3,\text{mod}}^{\text{eff}}(t) = \phi_m\,c(t) \tag{10}$$

with ϕ_m being the phase modulation depth and $c(t)$ the modulation waveform with $|c(t)| \le 1$. For the modulation waveforms generally used in such applications, $c(t)$ is assumed to be an odd and periodic function of period T_m whose spectrum contains only odd harmonics of the modulation frequency $f_m = 1/T_m$. Then, from (5), the global phase due to the modulation becomes

$$\Phi_{L,\text{mod}}(t) = \phi_m\,c(t - T_{det}). \tag{11}$$

Finally, the correction signal $e(t)$ applied to the CLO oscillator generating the frequency $\omega_c(t)$ is obtained by synchronously demodulating the output signal $I_e(t)$ of the gyroscope and then by applying the output signal of the synchronous detector $s(t)$ to the servo-loop filter.

2.3 Correction signal of the CLO

In order to evaluate the specific contribution of the intermodulation noise to the rotation rate measurement instability, we do not take into account the shot-noise of the atomic beam and we also assume that the servo-loop adds no excess noise. We consider only the main noise

sources identified on this type of gyroscope. Namely, the vibration (acceleration) noise of the retroreflecting mirror, the phase noise of the free running Raman local oscillator (RLO) used to generate the microwave frequency ω_0 of the Raman transition and the laser phase noise of the Raman fields characterized by their power spectral densities $S_a^{\mathrm{M}}(f)$, $S_\phi^{\mathrm{RLO}}(f)$ and $S_\phi^{\mathrm{L}}(f)$ respectively. For completeness, we will also take into account the phase noise of the free running CLO, as introduced in (7), which is characterized by the power spectral density $S_\phi^{\mathrm{CLO}}(f)$.

We can write down the total phase of the gyroscope as the sum of two terms

$$\Phi(t) = \Phi_{\mathrm{rot}}(t) + \Phi_{\mathrm{L}}(t) \tag{12}$$

where the phase due to rotation reads for an assumed perfect geometry of the interferometer

$$\Phi_{\mathrm{rot}}(t) = 2\,\frac{L^2}{v}\,k_{\mathrm{eff}}\,\Omega_z(t) \tag{13}$$

$\Omega_z(t)$ being the magnitude of the rotation vector component perpendicular to the assumed horizontal interferometer plane.

The global phase $\Phi_{\mathrm{L}}(t)$ due to the laser fields can be expressed from (8), (9) and (11) as

$$\Phi_{\mathrm{L}}(t) = \Phi_{\mathrm{L,c}} + \Phi_{\mathrm{L,mod}}(t) + \delta\Phi_{\mathrm{L,c}}(t) + \delta\Phi_{\mathrm{L}}(t). \tag{14}$$

The constant Raman frequency ω_0 gives rise to a nul contribution to $\Phi_{\mathrm{L}}(t)$ and the frequency fluctuations $\delta\omega_{\mathrm{RLO}}(t)$ of the RLO oscillator are included in the random part $\delta\Phi_{\mathrm{L}}(t)$ grouping also together the phase fluctuations of the laser fields due to the mirror vibrations and the laser phase noises.

The time-dependent response of the gyroscope's output signal to the phase modulation, which is proportional to the time-dependent probability (1), is given by the current of a photodetector measuring the fluorescence light at the detection and may now be written as

$$I_e(t) = \frac{I_0}{2}\Big\{1 - C\cos\big(\Phi_{\mathrm{rot}}(t) + \Phi_{\mathrm{L,c}} + \Phi_{\mathrm{L,mod}}(t) + \delta\Phi_{\mathrm{L,c}}(t) + \delta\Phi_{\mathrm{L}}(t)\big)\Big\} \tag{15}$$

where $I_0/2$ is the signal on the side of the interference fringes and we have admitted, in order to keep the model simple, that the photodetector is an ideal detector with unlimited bandwidth.

In the following, we restrict our analysis to the steady-state regime of the gyroscope where the inertial phase is controlled by the servo-loop. We assume that the time scale of the variations of the rotation rate $\Omega_z(t)$ is much slower than the time constant of the servo-loop. In that case the inertial phase $\Phi_{\mathrm{rot}}(t)$ appears as being a constant phase Φ_{rot} and the rotation rate a constant value Ω_z to the servo-loop which will keep the phase difference $\Phi_{\mathrm{rot}} + \Phi_{\mathrm{L,c}}$ equal to zero permanently. Thus, we have a precise relationship between the rotation rate Ω_z and the angular frequency ω_{c} that can be deduced from (8) and (13) to be

$$\Omega_z = \frac{\omega_{\mathrm{c}}}{k_{\mathrm{eff}} L}. \tag{16}$$

So, in closed loop operation, the remaining total effective phase is only due to the phase modulation and to the small time-dependent phase fluctuations of the laser fields due to the vibrations of the mirror and the phase noise of the oscillators. The standard deviations of $\delta\Phi_{\mathrm{L,c}}(t)$ and $\delta\Phi_{\mathrm{L}}(t)$ are much smaller than ϕ_{m} which is usually of the order of $\pi/2$ radian

$$\delta\Phi_{\mathrm{L,c}}(t), \delta\Phi_{\mathrm{L}}(t) \ll \phi_{\mathrm{m}}. \tag{17}$$

Then, we can expand (15) up to the first order of the ratio $(\delta\Phi_{\mathrm{L,c}}(t) + \delta\Phi_{\mathrm{L}}(t))/\phi_{\mathrm{m}}$ to get

$$I_e(t) \cong \frac{I_0}{2}\Big\{1 - C\cos\big(\Phi_{\mathrm{L,mod}}(t)\big)\Big\} + \frac{I_0}{2}\,C\,\big(\delta\Phi_{\mathrm{L,c}}(t) + \delta\Phi_{\mathrm{L}}(t)\big)\sin\big(\Phi_{\mathrm{L,mod}}(t)\big). \tag{18}$$

This signal is then synchronously demodulated at the frequency f_{m} and lowpass filtered with a cut-off frequency $f_{\mathrm{s}} \ll f_{\mathrm{m}}$. Since the spectrum of the periodic function $c(t)$ contains only odd harmonics of f_{m}, it follows that the spectrum of $\cos\left(\Phi_{\mathrm{L,mod}}(t)\right)$ and of $\sin\left(\Phi_{\mathrm{L,mod}}(t)\right)$ contains only even and odd harmonics respectively. Therefore, only the last term of (18) will provide the error signal.

If $d(t)$ denotes the demodulation waveform of the synchronous detector, the signal at its output is given by

$$s(t) = \frac{I_0}{2}\,C\big(\delta\Phi_{\mathrm{L,c}}(t) + \delta\Phi_{\mathrm{L}}(t)\big)\sin\big(\Phi_{\mathrm{L,mod}}(t)\big) \times d(t - T_{\mathrm{d}}) * h_s(t) \tag{19}$$

where the symbol $*$ indicates the convolution product. T_{d} is the delay time of the demodulation waveform and $h_s(t)$ is the impulse response of the lowpass filter of the synchronous detector. The correction signal $e(t)$ applied to the CLO is obtained after passing through a loop filter

$$e(t) = s(t) * h_F(t) \tag{20}$$

where $h_F(t)$ is the impulse response of a linear loop filter F. Equations (19) and (20) are the basic relationships of our model. They will be analyzed in Section 3 in order to get the power spectral density of the CLO frequency fluctuations in closed loop.

3 Power spectral density of the CLO frequency fluctuations in closed loop

We are now interested to calculate the spectrum of the correction signal $e(t)$ defined by (20). The signal $s(t)$ at the output of the synchronous detector is composed of two parts:

– a random part $\delta\Phi_{\mathrm{L,c}}(t) + \delta\Phi_{\mathrm{L}}(t)$ depending on the phase fluctuations $\delta\Phi_{\mathrm{L,c}}(t)$ due to the CLO phase noise and on the laser fields phase fluctuations $\delta\Phi_{\mathrm{L}}(t)$. We assume in the following that the random processes $\delta\Phi_{\mathrm{L,c}}(t)$ and $\delta\Phi_{\mathrm{L}}(t)$ are stationary and of zero mean value;

– a deterministic part $\sin\left(\Phi_{\mathrm{L,mod}}(t)\right) d(t-T_{\mathrm{d}})$ which depends on the modulation-demodulation process.

Let us start by calculating the two-sided power spectral density $S'_{\delta\Phi_{\mathrm{L}}}(f)$ of the random part $\delta\Phi_{\mathrm{L}}(t)$. For that, we take into account, as shown in Figure 3, the time delay $T_{\mathrm{del}} = 2\,l/c$ of the phase fluctuations $\delta\phi_{\mathrm{L2}}(t)$ of the retroreflected laser beam L2 together with the fluctuations $\delta l(t)$ of the mirror distance due to vibrations. l being the distance between the mirror and the atom's trajectory and c denotes the speed of light. Since the three Raman beams are coming from the same laser field and that we have only one large retroreflecting mirror, the random parts $\delta\phi_i^{\mathrm{eff}}(t)$ for $i = 1, 2$ and 3 of each individual Raman interaction can be written at the lowest order as

$$\delta\phi_i^{\mathrm{eff}}(t) = \delta\phi_{\mathrm{L1}}(t) - \delta\phi_{\mathrm{L2}}(t - T_{\mathrm{del}}) + 2\,k_2\,\delta l(t - T_{\mathrm{del}}/2) \quad (21)$$

where $\delta\phi_{\mathrm{L1}}(t)$ and $\delta\phi_{\mathrm{L2}}(t)$ are the phase fluctuations of the laser beams L1 and L2 respectively and k_2 is the wave number of the laser beam L2. Inserting (21) into (5), $\delta\Phi_{\mathrm{L}}(t)$ can be expressed by a sum of three terms

$$\delta\Phi_{\mathrm{L}}(t) = \delta\Phi_{\mathrm{RLO}}(t) + \delta\Phi_{\mathrm{L2}}(t) + \delta\Phi_{\mathrm{M}}(t) \quad (22)$$

$\delta\Phi_{\mathrm{RLO}}(t)$ is the instantaneous phase fluctuation due to the RLO phase noise that can be written as

$$\delta\Phi_{\mathrm{RLO}}(t) = q\,\delta\phi_{\mathrm{RLO}}(t) * h_{\mathrm{RLO}}(t) \quad (23)$$

where $\delta\phi_{\mathrm{RLO}}(t)$ is a random function representing the RLO phase fluctuations and q is the multiplying factor of the RLO frequency ω_{RLO}. The time function $h_{\mathrm{RLO}}(t)$ is given by

$$h_{\mathrm{RLO}}(t) = \delta(t - 2T - T_{\mathrm{det}}) - 2\,\delta(t - T - T_{\mathrm{det}}) + \delta(t - T_{\mathrm{det}}) \quad (24)$$

with $\delta(t)$ being the Dirac impulse function of time.

$\delta\Phi_{\mathrm{L2}}(t)$ represents the instantaneous phase fluctuation due to the retroreflected laser beam L2 and can be written in the same way as

$$\delta\Phi_{\mathrm{L2}}(t) = \delta\phi_{\mathrm{L2}}(t) * h_{\mathrm{L2}}(t) \quad (25)$$

with

$$\begin{aligned} h_{\mathrm{L2}}(t) = {} & \delta(t - 2T - T_{\mathrm{det}} - T_{\mathrm{del}}/2) \\ & - \delta(t - 2T - T_{\mathrm{det}} + T_{\mathrm{del}}/2) \\ & - 2\,\delta(t - T - T_{\mathrm{det}} - T_{\mathrm{del}}/2) \\ & + 2\,\delta(t - T - T_{\mathrm{det}} + T_{\mathrm{del}}/2) \\ & + \delta(t - T_{\mathrm{det}} - T_{\mathrm{del}}/2) - \delta(t - T_{\mathrm{det}} + T_{\mathrm{del}}/2) \end{aligned} \quad (26)$$

$\delta\Phi_{\mathrm{M}}(t)$ corresponds to the instantaneous phase fluctuation due to the mirror vibrations. It can be written in a good approximation as

$$\delta\Phi_{\mathrm{M}}(t) = k_{\mathrm{eff}}\,\delta a_{\mathrm{M}}(t) * h_{\mathrm{M}}(t) \quad (27)$$

with $\delta a_{\mathrm{M}}(t)$ being the fluctuations of the mirror acceleration $a_{\mathrm{M}}(t)$ and $\ddot{h}_{\mathrm{M}}(t) = h_{\mathrm{RLO}}(t)$ where the dots stand for time derivative.

Assuming that there are no correlations between the mirror vibrations, the laser fields phase noise and the RLO phase noise, the autocorrelation function $R_{\delta\Phi_{\mathrm{L}}}(\tau)$ of (22) is simply

$$R_{\delta\Phi_{\mathrm{L}}}(\tau) = R_{\delta\Phi_{\mathrm{RLO}}}(\tau) + R_{\delta\Phi_{\mathrm{L2}}}(\tau) + R_{\delta\Phi_{\mathrm{M}}}(\tau) \quad (28)$$

with the individual autocorrelation functions $R_{\delta\Phi_\beta}(\tau)$ for $\beta =$ RLO, L2 or M of the form

$$R_{\delta\Phi_\beta}(\tau) = k_\beta^2\,R_{\delta x_\beta}(\tau) * h_\beta(-\tau) * h_\beta(\tau) \quad (29)$$

where $R_{\delta x_\beta}(\tau)$ is the autocorrelation function of the random variable $\delta x_\beta(t)$ and k_β is a constant. According to the Wiener-Khintchine theorem [15], the two-sided power spectral density of $\delta\Phi_{\mathrm{L}}(t)$ is obtained by taking the Fourier transform of $R_{\delta\Phi_{\mathrm{L}}}(\tau)$. We get an expression of the following form for the power spectral density of each term of the type (29)

$$S'_{\delta\Phi_\beta}(f) = k_\beta^2\,|H_\phi^\beta(f)|^2\,S_x^{'\beta}(f) \quad (30)$$

where $H_\phi^\beta(f)$ is the Fourier transform of $h_\beta(t)$ and $S_x^{'\beta}(f)$ is the two-sided power spectral density of the random variable $\delta x_\beta(t)$. Finally, we obtain for the two-sided power spectral density of $\delta\Phi_{\mathrm{L}}(t)$ the following expression

$$\begin{aligned} S'_{\delta\Phi_{\mathrm{L}}}(f) = {} & 16\,q^2\,|H_\phi^{\mathrm{RLO}}(f)|^2\,S_\phi^{'\mathrm{RLO}}(f) + 64\,|H_\phi^{\mathrm{L}}(f)|^2 \\ & \times S_\phi^{'\mathrm{L}}(f) + |H_\phi^{\mathrm{M}}(f)|^2\,k_{\mathrm{eff}}^2\,T^4\,S_a^{'\mathrm{M}}(f) \end{aligned} \quad (31)$$

with the corresponding normalized and dimensionless transfer functions

$$\begin{aligned} H_\phi^{\mathrm{RLO}}(f) &= -\sin^2(\pi f T)\,e^{-i2\pi f(T+T_{\mathrm{det}})} \\ H_\phi^{\mathrm{L}}(f) &= i\sin(\pi f T_{\mathrm{del}})\sin^2(\pi f T)\,e^{-i2\pi f(T+T_{\mathrm{det}})} \\ H_\phi^{\mathrm{M}}(f) &= \mathrm{sinc}^2(\pi f T)\,e^{-i2\pi f(T+T_{\mathrm{det}})} \end{aligned} \quad (32)$$

where $\mathrm{sinc}(x) = \sin(x)/x$.

The fluctuation of the phase due to the frequency offset can readily be obtained, as a function of the phase fluctuations $\delta\phi_{\mathrm{CLO}}(t)$ of the free running CLO, from (9) to be

$$\delta\Phi_{\mathrm{L,c}}(t) = q_{\mathrm{c}}\,\delta\phi_{\mathrm{CLO}}(t) * h_{\mathrm{c}}(t) \quad (33)$$

with $h_{\mathrm{c}}(t)$ given by

$$h_{\mathrm{c}}(t) = \delta(t - 2T - T_{\mathrm{det}}) - \delta(t - T_{\mathrm{det}}). \quad (34)$$

The two-sided power spectral density of $\delta\Phi_{\mathrm{L,c}}(t)$ is then

$$S'_{\delta\Phi_{\mathrm{L,c}}}(f) = 4\,q_{\mathrm{c}}^2\,|H_\phi^{\mathrm{CLO}}(f)|^2\,S_\phi^{'\mathrm{CLO}}(f) \quad (35)$$

with the normalized transfer function

$$H_\phi^{\mathrm{CLO}}(f) = -i\sin(2\pi f T)\,e^{-i2\pi f(T+T_{\mathrm{det}})}. \quad (36)$$

Now, we turn to the deterministic part of (19). Let $a(t)$ be the deterministic part of the output signal of the synchronous detection

$$a(t) = \sin\left(\Phi_{\mathrm{L,mod}}(t)\right) d(t - T_{\mathrm{d}}). \quad (37)$$

As the spectrum of the demodulation waveform $d(t)$ is assumed to contain only odd harmonics of the modulation frequency $f_{\rm m}$, the spectrum of $a(t)$ will contain even harmonics only. Let us also define the Fourier series development of $a(t)$

$$a(t) = c_0 + \sum_{k=1}^{+\infty} c_{2k}\, e^{i4k\pi f_{\rm m} t} + c_{2k}^{*}\, e^{-i4k\pi f_{\rm m} t} \tag{38}$$

where the star denotes the complex conjugate. The coefficients c_{2k} are calculable from the knowledge of the modulation and demodulation waveforms. Expressions for these coefficients are given in Appendix A for a square wave phase modulation and a square demodulation waveform. Its autocorrelation function $R_a(\tau)$ is then the following

$$R_a(\tau) = c_0^2 + \sum_{k=1}^{+\infty} |c_{2k}|^2 \left(e^{i4k\pi f_{\rm m}\tau} + e^{-i4k\pi f_{\rm m}\tau}\right). \tag{39}$$

The two-sided power spectral density follows immediately

$$S'_a(f) = c_0^2\, \delta(f) + \sum_{k=1}^{+\infty} |c_{2k}|^2 \left\{\delta(f - 2kf_{\rm m}) + \delta(f + 2kf_{\rm m})\right\} \tag{40}$$

with $\delta(f)$ being the Dirac impulse function of frequency.

From (19), the autocorrelation function of the signal $s(t)$ at the output of the synchronous detector is given by

$$\begin{aligned} R_s(\tau) = {} & \frac{I_0^2\, C^2}{4} \left(R_{\delta\Phi_{\rm L,c}}(\tau) + R_{\delta\Phi_{\rm L}}(\tau)\right) \\ & \times R_a(\tau) * h_s(-\tau) * h_s(\tau) \end{aligned} \tag{41}$$

since $\delta\Phi_{\rm L,c}(t)$, $\delta\Phi_{\rm L}(t)$ and $a(t)$ are independent variables [16]. The two-sided power spectral density of $s(t)$ is then readily obtained as

$$S'_s(f) = \frac{I_0^2\, C^2}{4} \left|H_s(f)\right|^2 \left(S'_{\delta\Phi_{\rm L,c}}(f) + S'_{\delta\Phi_{\rm L}}(f)\right) * S'_a(f) \tag{42}$$

where $H_s(f)$ is the Fourier transform of the lowpass filter impulse response $h_s(t)$ of the synchronous detector. From (20), the two-sided power spectral density of the correction signal $e(t)$ may be written

$$S'_e(f) = |G(f)|^2 \left(S'_{\delta\Phi_{\rm L,c}}(f) + S'_{\delta\Phi_{\rm L}}(f)\right) * S'_a(f) \tag{43}$$

where we have put

$$|G(f)|^2 = \frac{I_0^2\, C^2}{4} \left|H_F(f)\right|^2 \left|H_s(f)\right|^2 \tag{44}$$

with $H_F(f)$ being the Fourier transform of the impulse response $h_F(t)$ of the loop filter F. Inserting (31), (35) and (40) into (43), we obtain the following expression

$$\begin{aligned} S'_e(f) = {} & |G(f)|^2\, c_0^2 \left\{16\, q^2 |H_\phi^{\rm RLO}(f)|^2 S_\phi^{'\rm RLO}(f)\right. \\ & + 64\, |H_\phi^{\rm L}(f)|^2\, S_\phi^{'\rm L}(f) + |H_\phi^{\rm M}(f)|^2\, k_{\rm eff}^2\, T^4\, S_a^{'\rm M}(f) \\ & \left. + 4\, q_{\rm c}^2\, |H_\phi^{\rm CLO}(f)|^2\, S_\phi^{'\rm CLO}(f)\right\} + |G(f)|^2 \sum_{k=1}^{+\infty} |c_{2k}|^2 \\ & \times \Big\{16\, q^2\, |H_\phi^{\rm RLO}(f - 2kf_{\rm m})|^2\, S_\phi^{'\rm RLO}(f - 2kf_{\rm m}) \\ & + 64\, |H_\phi^{\rm L}(f - 2kf_{\rm m})|^2\, S_\phi^{'\rm L}(f - 2kf_{\rm m}) \\ & + |H_\phi^{\rm M}(f - 2kf_{\rm m})|^2\, k_{\rm eff}^2\, T^4\, S_a^{'\rm M}(f - 2kf_{\rm m}) \\ & + 4\, q_{\rm c}^2\, |H_\phi^{\rm CLO}(f - 2kf_{\rm m})|^2\, S_\phi^{'\rm CLO}(f - 2kf_{\rm m}) \\ & + \text{terms with } f - 2kf_{\rm m} \rightarrow f + 2kf_{\rm m}\Big\}. \end{aligned} \tag{45}$$

The spectral density of the correction signal $e(t)$ is composed of two parts. The first one which contains only the Fourier frequency f corresponds to the fluctuations coming from the different noise sources filtered through the gyroscope and the servo-loop. The second one, which contains all the even multiples of $f_{\rm m}$, corresponds to a spurious fluctuation generated by downconversion, during the demodulation process, of all the noise components at higher harmonics of the modulation frequency. This is the aliased part of the spectrum due in this case to the intermodulation effect.

The frequency fluctuations of the locked compensation local oscillator (LCLO) used to generate the frequency offset $\omega_{\rm c}$ can be deduced from the loop equation in time domain

$$\delta\omega_{\rm LCLO}(t) = \delta\omega_{\rm CLO}(t) + K_{\rm CLO}\, e(t) \tag{46}$$

where $K_{\rm CLO}$ is a characteristic constant of the quartz oscillator. To solve easily for the CLO frequency spectrum in closed loop, we assume that the lowpass filter of the synchronuous detector is an ideal lowpass filter whose transfer function is

$$|H_s(f)| = \begin{cases} 1 & |f| < f_s \\ 0 & |f| \geq f_s \end{cases} \tag{47}$$

with a cut-off frequency $f_s \ll f_{\rm m}$, which is usually the case in synchronous detection, and that $f_s \ll f_{\rm i}$ where $f_{\rm i} = 1/2T$ is the interrogation frequency of the Mach-Zehnder interrogation. We are, in this analysis, only interested by the intermodulation part of the spectrum (45). Then, the corresponding power spectral density of the LCLO frequency fluctuations is given, in the limit of a high loop filter gain $|H_F(f)| \gg 1$ and introducing one-sided

power spectral densities, by

$$S_\omega^{\mathrm{LCLO}}(f) \cong 2\sum_{k=1}^{+\infty}\frac{|c_{2k}|^2}{c_0^2} \times\left\{\frac{4\,q^2}{q_\mathrm{c}^2\,T^2}\frac{|H_\phi^{\mathrm{RLO}}(2kf_\mathrm{m})|^2}{|H_\omega^{\mathrm{CLO}}(0)|^2}\,S_\phi^{\mathrm{RLO}}(2kf_\mathrm{m}) + \frac{16}{q_\mathrm{c}^2\,T^2}\frac{|H_\phi^{\mathrm{L}}(2kf_\mathrm{m})|^2}{|H_\omega^{\mathrm{CLO}}(0)|^2}\,S_\phi^{\mathrm{L}}(2kf_\mathrm{m}) + \frac{1}{T^2}\frac{|H_\phi^{\mathrm{CLO}}(2kf_\mathrm{m})|^2}{|H_\omega^{\mathrm{CLO}}(0)|^2}\,S_\phi^{\mathrm{CLO}}(2kf_\mathrm{m}) + \frac{1}{4\,q_\mathrm{c}^2}\,k_\mathrm{eff}^2\,T^2\,\frac{|H_\phi^{\mathrm{M}}(2kf_\mathrm{m})|^2}{|H_\omega^{\mathrm{CLO}}(0)|^2}\,S_a^{\mathrm{M}}(2kf_\mathrm{m})\right\} \tag{48}$$

for $f < f_s$ and with the normalized and dimensionless CLO transfer function for frequency

$$H_\omega^{\mathrm{CLO}}(f) = -\,\mathrm{sinc}\,(2\pi fT)\;e^{-i2\pi f(T+T_\mathrm{det})}. \tag{49}$$

4 Result: Allan variance of the rotation rate

Now, we can compute the Allan variance of the rotation rate fluctuations, due to the intermodulation noises, for the gyroscope in closed loop. As the resulting intermodulation noise is a white frequency noise in the bandpass of the servo-loop, the asymptotic Allan variance of ω_c is readily obtained, for a measurement time τ, by the simple expression

$$\sigma_{\omega_\mathrm{c}}^2(\tau) \cong \frac{\tau^{-1}}{2}\,q_\mathrm{c}^2\,S_\omega^{\mathrm{LCLO}}(0). \tag{50}$$

Finally, with the relation (16), we get for the Allan variance of Ω_z the following expression

$$\sigma_{\Omega_z}^2(\tau,f_\mathrm{m}) \cong \frac{\tau^{-1}}{L^2}\sum_{k=1}^{+\infty}\frac{|c_{2k}|^2}{c_0^2}\left\{\frac{1}{k_\mathrm{eff}^2T^2}\left[\frac{4\omega_0^2}{\omega_{\mathrm{RLO}}^2}\sin^4(2k\pi f_\mathrm{m}T) \times S_\phi^{\mathrm{RLO}}(2kf_\mathrm{m}) + 16\,\sin^2(2k\pi f_\mathrm{m}T_\mathrm{del})\,\sin^4(2k\pi f_\mathrm{m}T) \times S_\phi^{\mathrm{L}}(2kf_\mathrm{m}) + \frac{\omega_\mathrm{c}^2}{\omega_{\mathrm{CLO}}^2}\,\sin^2(4k\pi f_\mathrm{m}T)\;S_\phi^{\mathrm{CLO}}(2kf_\mathrm{m})\right] + \frac{1}{4}\,T^2\,\mathrm{sinc}^4(2k\pi f_\mathrm{m}T)\;S_a^{\mathrm{M}}(2kf_\mathrm{m})\right\} \tag{51}$$

where we have stressed that the modulation frequency is a free parameter. This formula is the basic result that we will use to analyze the intermodulation noises in a Mach-Zehnder gyroscope.

We observe that the Allan deviation is inversely proportional to the distance L between two successive Raman beams which is the only global scaling factor that appears for a spatial-domain continuous gyroscope. The formula (51) is a sum of four terms, each term corresponding to a different source of noise and is composed of three multiplying factors if one excepts the constant factors. The first factor, which contain the Fourier coefficients c_{2k}, represents the effect of the modulation-demodulation process used to generate the correction signal $e(t)$. It depends on the type of the waveforms used for the modulation and demodulation and generally on the modulation frequency. Thus, the model allows us to compare the effect of different modulation-demodulation schemes on the sensitivity of the gyroscope. The second factor, containing the transfer functions, describes the filtering effect of the gyroscope for the corresponding noise and the last factor, the power spectral densities, characterizes the different sources of noise as said before.

5 Discussion

We will now discuss in more details the result (51) for both a pulsed and a continuous mode of operation. After that, we will also extend the result to the case of a real continuous atomic beam having a velocity distribution.

5.1 Pulsed operation of the gyroscope

With our model, we can also easily take into account a pulsed mode of operation of the gyroscope. The periodic availability of the correction signal $e(t)$ can be taken into account by a periodic sampling, with the launching period T_L, of the assumed constant intensity I_0 of the signal $e(t)$ corresponding to a constant atomic beam density. We can then replace I_0 in (15) by its pulsed counterpart

$$I_{0\mathrm{p}} = I_0\sum_{k=-\infty}^{+\infty}\delta(t-k\,T_\mathrm{L}) \tag{52}$$

assuming infinitesimally-short pulses of atom density. Doing again the spectral analysis of the so-defined output signal, we find for the Allan variance

$$\sigma_{\Omega_z}^2(\tau,f_\mathrm{L}) \cong \frac{\tau^{-1}}{L^2}\sum_{k=1}^{+\infty}\left\{\frac{1}{k_\mathrm{eff}^2T^2}\left[\frac{4\omega_0^2}{\omega_{\mathrm{RLO}}^2}\sin^4(k\pi f_\mathrm{L}T) \times S_\phi^{\mathrm{RLO}}(kf_\mathrm{L}) + 16\,\sin^2(k\pi f_\mathrm{L}T_\mathrm{del})\,\sin^4(k\pi f_\mathrm{L}T)\;S_\phi^{\mathrm{L}}(kf_\mathrm{L}) + \frac{\omega_\mathrm{c}^2}{\omega_{\mathrm{CLO}}^2}\,\sin^2(2k\pi f_\mathrm{L}T)\;S_\phi^{\mathrm{CLO}}(kf_\mathrm{L})\right] + \frac{1}{4}\,T^2\,\mathrm{sinc}^4(k\pi f_\mathrm{L}T)\;S_a^{\mathrm{M}}(kf_\mathrm{L})\right\} \tag{53}$$

where $f_\mathrm{L} = 1/T_\mathrm{L}$ is the launching frequency which is considered as a free parameter that can be varied in a given range. The resulting aliasing noise no longer depends on the detail of the modulation-demodulation process but the corresponding equivalent modulation frequency for a pulsed operation is now linked to the launching frequency by $f_\mathrm{m} = f_\mathrm{L}/2$.

The above formula is completely similar to the result already obtained, within the sensitivity function formalism, for the Allan variance of the interferometer phase fluctuations due to the Dick effect [17], thereby confirming the validity of our approach. The concept of the sensitivity function is well adapted to a pulsed mode of operation but attempts to apply it to a continuous mode of operation have shown difficulties [18,19] which are by-passed with our approach.

5.2 Cancellation of aliasing noises

5.2.1 Continuous operation of the gyroscope

The main consequence of the result (51) is that for specific modulation frequencies all the intermodulation noises can be filtered out, leading to a total cancellation of the Allan deviation due to the filtering properties of the Mach-Zehnder interrogation. Indeed, this is the case if all the even harmonics of the modulation frequency correspond to the common zeros of the transfer functions (32) and (36) or, in other words, if f_{m} is an integer multiple of f_{i} leading to the optimum modulation frequencies

$$f_{\mathrm{m}}^{(k)} = k f_{\mathrm{i}} \tag{54}$$

where $k \geq 1$ is an integer. Another remarkable feature is that this property is independent from the type of modulation-demodulation process used to get the correction signal. Therefore, it is possible, in addition, to choose the optimum scheme that will result in the lowest intermodulation noise level.

As shown in Appendix A, the function $a(t)$ in (37) remains always a constant and its Fourier coefficients c_{2k} in (38) are all equal to zero, except c_0, if we use a square wave phase modulation and a square wave demodulation in phase with the output signal. For the idealized continuous gyroscope considered here, this choice of modulation-demodulation scheme will even lead to a further cancellation of the overall intermodulation noise, through the vanishing of the Fourier coefficients c_{2k}, independent from the cancellation due to the filtering effect of the Mach-Zehnder interrogation. Moreover, this is true for any modulation frequency for a monokinetic beam and for a modulation applied to one Raman beam only. We are then expecting a suppression of the intermodulation noises, i.e. a cancellation of the Allan deviation (51), for any modulation frequency for a continous mode of operation with this optimum scheme.

Actually, for a real gyroscope with a non-monokinetic atomic beam for example, these two cancellations will not be complete. However, the level of the residual intermodulation noises should remain very low but should be dependent on the modulation frequency. In particular, we expect in that case a stronger cancellation around the first optimum modulation frequency $f_{\mathrm{m}}^{(1)} = f_{\mathrm{i}}$.

We can also note that the use of a square wave phase modulation on the last Raman beam is advantageous as it should not induce phase transients in the response of the interferometer.

5.2.2 Pulsed operation of the gyroscope

In the case of a pulsed mode of operation, the overall aliasing noise due to the Dick effect can also be cancelled for specific launching frequencies. From the relation (53) we can see that this is effectively the case for launching frequencies f_{L} that are an even multiple of f_{i}, leading to the optimum launching frequencies

$$f_{\mathrm{L}}^{(k)} = 2k f_{\mathrm{i}} \tag{55}$$

where $k \geq 1$ is an integer. As the rotation rate measurement instability does not depend on the modulation-demodulation scheme for a pulsed operation, we are expecting a strong cancellation only around these specific frequencies for a real gyroscope.

In the particular situation corresponding to the first launching frequency $f_{\mathrm{L}}^{(1)} = 2f_{\mathrm{i}}$, pulses of atoms are always present in the interferometer as when a pulse leaves the Raman beams 2 or 3, the next pulse enters the previous Raman beams 1 or 2. In fact, this mode of operation is equivalent to simulate a continuous beam from the point of view of aliasing. For launching frequencies $f_{\mathrm{L}} < f_{\mathrm{L}}^{(1)}$, the level of aliasing noise should be higher than for a continous mode of operation where atoms are permanently present in the interferometer.

5.3 Analytical results for pulsed operation

For a pulsed operation, it is possible to get analytical expressions for the Allan deviation of the rotation rate for some noise processes modelled by a power law.

5.3.1 Contributions of RLO, CLO and L terms

Let us first consider the important case of white phase noise. A look at the result (53) shows that for a white phase noise, the sums in each of the three first terms RLO, L and CLO does not converge leading to an infinite aliasing noise or Allan deviation. This is a consequence of the idealized modelization of the gyroscope considered here and, in particular, of infinitely short Raman interactions. As we have mentioned in Section 2, the finite interaction time of real Raman interactions introduces a lowpass filtering of the laser beams noise. To take into account, approximatively, the finite duration of the Raman interactions, we can simply lowpass-filter the phase fluctuations in the relation (5) by replacing the phases $\phi_i^{\mathrm{eff}}(t)$ for $i = 1, 2$ or 3 by

$$\phi_{i,\tau_{\mathrm{R}}}^{\mathrm{eff}}(t) = \phi_i^{\mathrm{eff}}(t) * h_{\tau_{\mathrm{R}}}(t) \tag{56}$$

where $h_{\tau_{\mathrm{R}}}(t)$ is the impulse response of the lowpass filter that simulates a Raman interaction of duration τ_{R}. This approximation is valid if we have $\tau_{\mathrm{R}}/T \ll 1$ which is usually the case in cold atom gyroscopes and is equivalent to

Table 1. Values of b_0^β and $f_0^\beta(\bar{n})$ for white phase noise.

β	b_0^β	$f_0^\beta(\bar{n})$
RLO	$0.82\,\frac{\omega_0}{\omega_{\rm RLO}}\left(h_0^{\rm RLO}\,\frac{T}{\tau_R}\right)^{1/2}$	$\eta(\bar{n})\,\bar{n}^{-1/2}$
CLO	$0.48\,\frac{\omega_{\rm c}}{\omega_{\rm CLO}}\left(h_0^{\rm CLO}\,\frac{T}{\tau_R}\right)^{1/2}$	$\xi_0(\bar{n})\,\bar{n}^{-1/2}$

replacing the module of the transfer functions $|H_\phi^\beta(f)|$ for $\beta =$ RLO, L or CLO by a new one

$$|H_{\phi,\tau_{\rm R}}^\beta(f)| = |H_\phi^\beta(f)|\,|H_{\tau_{\rm R}}(f)| \tag{57}$$

with $|H_{\tau_{\rm R}}(f)|$ being the module of the transfer function of a first-order lowpass filter given by

$$|H_{\tau_{\rm R}}(f)|^2 = \frac{1}{1+(f/f_{\tau_{\rm R}})^2} \tag{58}$$

with an effective cutoff frequency $f_{\tau_{\rm R}} = \sqrt{3}/12\,\tau_{\rm R}$ according to [17].

Now we can compute the Allan deviation (53). It can be expressed as a function of the mean number of atom pulses being interrogated $\bar{n} = f_{\rm L}/f_{\rm i}$ by

$$\sigma_{\Omega_z,\alpha}^\beta(\bar{n},\tau) = \frac{b_\alpha^\beta}{k_{\rm eff}\,L\,T}\;f_\alpha^\beta(\bar{n})\;\tau^{-1/2} \tag{59}$$

where $\beta =$ RLO, L or CLO and α describes the type of power law frequency dependence of the phase noise given by $S_{\phi,\alpha}^\beta(f) = h_\alpha^\beta f^\alpha$.

For a white phase noise $\alpha = 0$, we give in Table 1 an approximate value of the coefficients b_0^β for the terms $\beta =$ RLO and CLO together with the corresponding functions $f_0^\beta(\bar{n})$. We have omitted the term $\beta =$ L as the spectrum of the lasers $S_\phi^{\rm L}(f)$ is assumed to contain mainly white frequency noise. The functions $\eta(\bar{n})$ and $\xi_0(\bar{n})$ are given in good approximation for $\bar{n} > 0$ by

$$\eta(\bar{n}) = \begin{cases} 1 & \bar{n} \neq 2k \\ 0 & \bar{n} = 2k \end{cases} \tag{60}$$

and

$$\xi_0(\bar{n}) = \begin{cases} 1 & \bar{n} \neq k \\ 0 & \bar{n} = k \end{cases} \tag{61}$$

where $k \geq 1$ is an integer. In fact, the cancellation of the functions $\eta(\bar{n})$ and $\xi_0(\bar{n})$, around $\bar{n} = 2k$ or k respectively, is very sharp but not infinitesimally narrow. The width of the cancellation depends on the cutoff frequency $f_{\tau_{\rm R}}$ of the lowpass filter, i.e. on the Raman pulse duration $\tau_{\rm R}$. We give below the full width at half hight $\Delta\bar{n}_k$ of the kth cancellation's dip of the functions $\eta(\bar{n})$ and $\xi_0(\bar{n})$ for $\tau_{\rm R} \ll T$

$$\Delta\bar{n}_k \cong \begin{cases} 4.6\,k\,\tau_{\rm R}/T & \text{for } \eta(\bar{n}) \\ 0.86\,k\,\tau_{\rm R}/T & \text{for } \xi_0(\bar{n}). \end{cases} \tag{62}$$

Table 2. Values of $p_\gamma(x)$.

γ	$p_\gamma(x)$
1/2	1
3/2	$1 - \frac{3}{4}\,x$
2	$1 - \frac{7}{5}\,x + \frac{1}{2}x^2$

Table 3. Values of b_{-2}^β and $f_{-2}^\beta(\bar{n})$ for white frequency noise.

β	b_{-2}^β	$f_{-2}^\beta(\bar{n})$
RLO	$\pi\,\frac{\omega_0}{\omega_{\rm RLO}}\left(2h_{-2}^{\rm RLO}\right)^{1/2}T$	$\zeta_{1/2}(\bar{n})\,\bar{n}^{-1/2}$
L	$5.2\left(h_{-2}^{\rm L}\,\frac{T}{\tau_R}\right)^{1/2}T_{\rm del}$	$f_0^{\rm RLO}(\bar{n})$
CLO	$\pi\,\frac{\omega_{\rm c}}{\omega_{\rm CLO}}\left(2h_{-2}^{\rm CLO}\right)^{1/2}T$	$\xi_{-2}(\bar{n})\,\bar{n}^{-1/2}$

For usual Raman pulses this width is very narrow as it can be seen in the zooms, around $\bar{n} = 2$, in Figures 4 and 5 obtained for $\tau_{\rm R} = 5\,\mu$s and $T = 23\,$ms corresponding to typical values for a cold atom gyroscope. For other values of $\bar{n}$, we can see in Table 1 that the level of aliasing noise depends also on $\tau_{\rm R}$. To minimize it, one should increase the pulses's duration in order to reduce the cutoff frequency of the equivalent lowpass filter. But, for a real gyroscope, it will decrease the contrast of the interference fringes since the Raman transitions are very selective with respect to the transverse velocity of the atom's motion. In practice, the choice of the pulses's length will result in a trade-off between fringe contrast and level of aliasing noise.

We turn now to the case of a white frequency noise $\alpha = -2$. We give results only up to the first optimum launching frequency, i.e. $\bar{n} = 2$. Let $\zeta_\gamma(\bar{n})$ be the following function

$$\zeta_\gamma(\bar{n}) = \begin{cases} p_\gamma^{1/2}(\bar{n}) & 0 < \bar{n} \leq 1 \\ \left(\frac{2-\bar{n}}{\bar{n}}\right)^\gamma p_\gamma^{1/2}(2-\bar{n}) & 1 \leq \bar{n} \leq 2 \\ \left(\frac{\bar{n}-2}{\bar{n}}\right)^\gamma p_\gamma^{1/2}(\bar{n}-2) & 2 \leq \bar{n} \leq 3 \end{cases} \tag{63}$$

for $\gamma = 1/2$, $3/2$ and 2 where $p_\gamma(x)$ is a polynomia given in Table 2. The value of the coefficients b_{-2}^β and the functions $f_{-2}^\beta(\bar{n})$ are summarized in Table 3 where the function $\xi_{-2}(\bar{n})$ is defined by

$$\xi_{-2}(\bar{n}) = \begin{cases} (1-\bar{n})^{1/2} & 0 < \bar{n} \leq 1 \\ \left(\frac{2-\bar{n}}{\bar{n}}\right)^{1/2}(\bar{n}-1)^{1/2} & 1 \leq \bar{n} \leq 2 \\ \left(\frac{3-\bar{n}}{\bar{n}}\right)^{1/2}(\bar{n}-2)^{1/2} & 2 \leq \bar{n} \leq 3. \end{cases} \tag{64}$$

As the sum in (53) converges rapidly, the corresponding aliasing noise does not depend on the pulse length for usual values. Figures 4 and 5 show a plot of the functions $f_0^\beta(\bar{n})$ and $f_{-2}^\beta(\bar{n})$ for $\beta =$ RLO and CLO. It illustrates the filtering effect around the first optimum launching frequency ($\bar{n} = 2$) which cancels both white phase and frequency noises. As said previously, for a white phase noise this filtering is very sharp as it can be clearly seen in the zooms in the graphs.

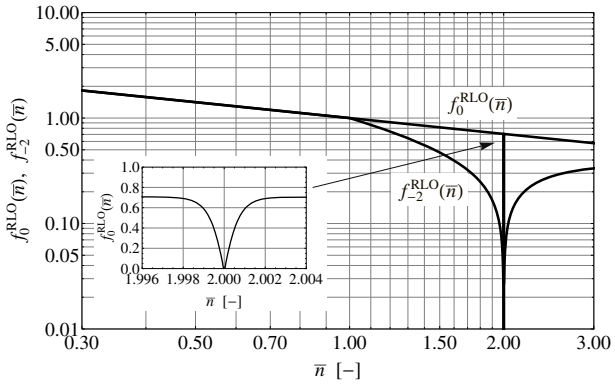

Fig. 4. Illustration of the filtering effect for a pulsed Mach-Zehnder interrogation for white phase and frequency noises of the local oscillator generating the Raman frequency ω_0. The graph represents a plot of the functions $f_0^{\mathrm{RLO}}(\bar{n})$ and $f_{-2}^{\mathrm{RLO}}(\bar{n})$ as a function of $\bar{n}$. It clearly shows the cancellation of the aliasing noises around the first optimum launching frequency $\bar{n} = 2$ and the zoom shows the sharpness of this cancellation for white phase noise.

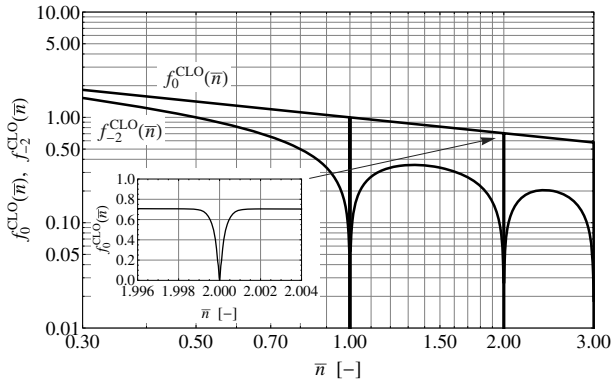

Fig. 5. Illustration of the filtering effect for a pulsed Mach-Zehnder interrogation for white phase and frequency noises of the local oscillator generating the offset frequency ω_c. The graph represents a plot of the functions $f_0^{\mathrm{CLO}}(\bar{n})$ and $f_{-2}^{\mathrm{CLO}}(\bar{n})$ as a function of $\bar{n}$ showing, in particular, the cancellation of the aliasing noises around the first optimum launching frequency $\bar{n} = 2$. This cancellation is very sharp as the zoom shows it.

5.3.2 Contribution of the M term

Concerning the vibration noise of the mirror, the corresponding Allan deviation can be expressed in a same way by

$$\sigma^{\mathrm{M}}_{\Omega_z,\alpha}(\bar{n},\tau) = \frac{b^{\mathrm{M}}_{\alpha}}{L}\, f^{\mathrm{M}}_{\alpha}(\bar{n})\ \tau^{-1/2} \tag{65}$$

where α describes the type of power law frequency dependence of the mirror acceleration noise $S^{\mathrm{M}}_{a,\alpha}(f) = h^{\mathrm{M}}_{\alpha} f^{\alpha}$. For the following three cases, $\alpha = 0$ (white acceleration noise), $\alpha = -2$ (random walk noise of acceleration) and $\alpha = 2$, the values of the coefficients b^{M}_{α} and the functions $f^{\mathrm{M}}_{\alpha}(\bar{n})$ are given in Table 4.

Due to the strong filtering of vibrations by the Mach-Zehnder interrogation, here also the corresponding aliasing noises do not depend on the pulse length. The behaviour of the functions $f^{\mathrm{M}}_{\alpha}(\bar{n})$ is showed around the first optimum launching frequency in Figure 6.

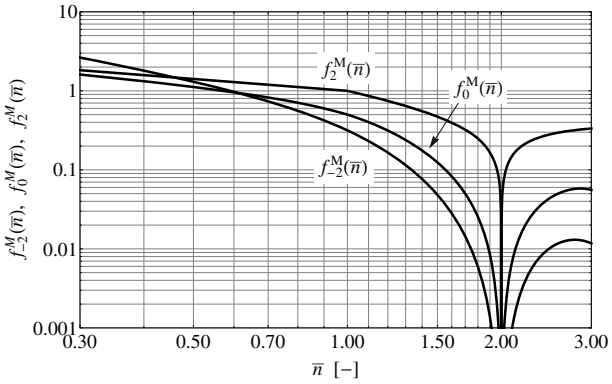

Fig. 6. Illustration of the filtering effect for a pulsed Mach-Zehnder interrogation for the different mirror vibration noise types considered. The graph represents a plot of the functions $f^{\mathrm{M}}_{-2}(\bar{n})$, $f^{\mathrm{M}}_{0}(\bar{n})$ and $f^{\mathrm{M}}_{2}(\bar{n})$ as a function of $\bar{n}$. It shows the strong cancellation of the aliasing noises due to vibrations around the first optimum launching frequency $\bar{n} = 2$.

Table 4. Values of b^{M}_{α} and $f^{\mathrm{M}}_{\alpha}(\bar{n})$ for $\alpha = -2, 0, 2$.

α	b^{M}_{α}	$f^{\mathrm{M}}_{\alpha}(\bar{n})$
-2	$\pi \left(\frac{1}{6} h^{\mathrm{M}}_{-2}\right)^{1/2} T^2$	$\zeta_2(\bar{n})\, \bar{n}^{-1}$
0	$\left(\frac{1}{6} h^{\mathrm{M}}_{0}\right)^{1/2} T$	$\zeta_{3/2}(\bar{n})\, \bar{n}^{-1/2}$
2	$\frac{1}{2\pi} \left(\frac{1}{2} h^{\mathrm{M}}_{2}\right)^{1/2}$	$f^{\mathrm{RLO}}_{-2}(\bar{n})$

5.3.3 Particular cases of operation

We observe that the Allan deviation diverges as $\propto \bar{n}^{-1/2}$ for a quasi-static pulsed operation ($\bar{n} \ll 1$) for all noise types considered here except for a random walk noise of vibration ($\alpha = -2$) where the divergence behaves as $\propto \bar{n}^{-1}$. Thus, for very slow pulsed operation, this type of noise is expected to provide the bigger contribution to the overall aliasing noise. On the contrary, if the gyroscope is operated near the first optimum launching frequency ($\bar{n} \cong 2$), all the noise components are efficiently filtered out except for the RLO white phase noise where the filtering effect is strongly dependent on the launching frequency around $\bar{n} = 2$. Only if the launching frequency corresponds exactly to the optimum frequency, will the cancellation of the white phase noise take place.

It means that for a real gyroscope, having a velocity distribution around the mean velocity of the atoms for example, this complete cancellation could not be realized for all the atoms leading to a residual aliasing noise that could be not negligible. The operation of a gyroscope at this particular launching frequency corresponds in fact to have always one pulse of atoms between two consecutive laser beams with each pulse spatially spaced from each other by the distance L. We can remark also that in the limit of a continuous beam, when $\bar{n}$ goes to infinity, all

the functions $f_\alpha^\beta(\bar{n})$ go to zero finding again that for a continuous operation the overall aliasing noise is totally cancelled.

5.4 Continuous operation with a non-monokinetic atomic beam

A direct comparison of the aliasing noise level of a pulsed gyroscope with the results obtained for a gyroscope in a continous mode of operation is not immediately possible. This is because we have considered an idealized gyroscope (monokinetic atomic beam among other things) where, in a continuous mode, the overall intermodulation noise is always zero for any modulation frequency as discussed in paragraph 5.2.1. To make possible a comparison, we now take into account a horizontal velocity distribution of the continuous atomic beam in order to estimate the residual intermodulation noise level. We assume a gaussian velocity distribution, of mean velocity $\bar{v}$, with a standard deviation σ_v related to the longitudinal beam temperature T_l by

$$\sigma_v = \left(\frac{k_\mathrm{B}\, T_l}{m_\mathrm{at}}\right)^{1/2} \tag{66}$$

where k_B is the Boltzmann constant and m_at is the mass of the atoms. Doing again the derivation of the Allan variance, we find

$$\sigma_{\Omega_z}^2(\tau, f_\mathrm{m}) \cong \frac{\tau^{-1}}{L^2} \sum_{k=1}^{+\infty} \left\{ \frac{1}{k_\mathrm{eff}^2\, \overline{T}^2} \left[\frac{4\,\omega_0^2}{\omega_\mathrm{RLO}^2} \frac{|C_{2k}^\mathrm{RLO}(2kf_\mathrm{m})|^2}{C_0^2} \right.\right.$$
$$\times\, S_\phi^\mathrm{RLO}(2kf_\mathrm{m}) + 16\, \frac{|C_{2k}^\mathrm{L}(2kf_\mathrm{m})|^2}{C_0^2}\, S_\phi^\mathrm{L}(2kf_\mathrm{m})$$
$$\left. + \frac{\omega_\mathrm{c}^2}{\omega_\mathrm{CLO}^2} \frac{|C_{2k}^\mathrm{CLO}(2kf_\mathrm{m})|^2}{C_0^2}\, S_\phi^\mathrm{CLO}(2kf_\mathrm{m}) \right]$$
$$\left. + \frac{1}{4}\, \overline{T}^2\, \frac{|C_{2k}^\mathrm{M}(2kf_\mathrm{m})|^2}{C_0^2}\, S_a^\mathrm{M}(2kf_\mathrm{m}) \right\} \tag{67}$$

where $\overline{T} = L\bar{v}^{-1}$ is the mean transit time. The expression of the coefficients C_0, $C_{2k}^\beta(f)$ for $\beta =$ RLO, L or CLO and $C_{2k}^\mathrm{M}(f)$ is given in Appendix B for a square wave phase modulation. They depend on the longitudinal temperature of the beam and on the modulation frequency.

As they are expressed by relatively complicated expressions, we have derived an approximate relation, valid for slow modulation frequencies ($f_\mathrm{m} < f_\mathrm{i}/2$ or $\bar{n} < 1$), which links together the Allan deviation of the rotation rate for a pulsed and a continuous mode of operation. It is given as a function of $\bar{n}$ and at the lowest order in $\sigma_v/\bar{v}$ by

$$\sigma_{\Omega_z}^\mathrm{cont}(f_\mathrm{m} = \bar{n} f_\mathrm{i}/2, \tau) \approx 2 \sqrt{\frac{2}{\pi}}\, \frac{L_\mathrm{det}}{L}\, \bar{n}\, \frac{\sigma_v}{\bar{v}}\, \sigma_{\Omega_z}^\mathrm{puls}(\bar{n}, \tau). \tag{68}$$

This expression shows that the residual intermodulation noise is proportional to the square root of the longitudinal temperature of the beam for very low temperatures and to the distance L_det between the last Raman beam and the detection. For a monokinetic beam ($T_l = 0$), we find again that the intermodulation noise is zero for any modulation frequency.

We remark also that, on the contrary to the pulsed case, for a quasi-static modulation ($f_\mathrm{m} \ll f_\mathrm{i}/2$ or $\bar{n} \ll 1$), the intermodulation noise is suppressed for all noise types considered in this paper except for a random walk noise of mirror vibrations ($\alpha = -2$) for which the level of intermodulation noise becomes a constant. This is due to the fact that for longer periods of modulation, the effect of the velocity distribution on the output signal of the gyroscope becomes relatively less important. In fact, the deterministic part $a(t)$ of the error signal approaches from a constant as it becomes more and more a product of two perfect square waveforms when the period of modulation increases. As a result, the module of the Fourier coefficients $|c_{2k}|$ of the Fourier development of $a(t)$ are going to zero as $\propto \bar{n}$ with increasing modulation period leading to a cancellation of the intermodulation noise except for a vibration noise of the type $h_{-2}^\mathrm{M} f^{-2}$ for which the Allan deviation diverges as $\propto \bar{n}^{-1}$. In that case the corresponding Allan deviation reads

$$\sigma_{\Omega_z}^\mathrm{cont}(f_\mathrm{m} \to 0, \tau) \approx 2 \sqrt{\frac{\pi}{3}\, h_{-2}^\mathrm{M}}\, L_\mathrm{det}\, \frac{\sigma_v}{\bar{v}^3}\, \tau^{-1/2} \tag{69}$$

for a continuous operation in the limit of a quasi-static modulation.

Let us now estimate the gain in stability that can be expected from the decrease of the intermodulation noise level thanks to a continuous operation of the gyroscope. To get realistic values, we use the data corresponding to the gyroscope described in [4] and we assume a longitudinal temperature of the atomic beam of $T_l = 50\,\mu$K, corresponding to a width of the velocity distribution of $\sigma_v \cong 7\,$cm/s for rubidium atoms. Taking $L_\mathrm{det} = 3\,$cm, $L = 6.5\,$cm and $\bar{v} = 2.8\,$m/s leads to a transit time $T \cong 23\,$ms and an interrogation frequency of $f_\mathrm{i} \cong 22\,$Hz. For comparison, we assume a pulsed operation of the gyroscope with a typical launching period of $T_\mathrm{L} \cong 1\,$s, which corresponds to $\bar{n} \cong 0.045$. From (68), we find that the Allan deviation for a continuous mode of operation, at the modulation frequency of $f_\mathrm{m} = 0.5\,$Hz, is less than 10^{-3} that for a pulsed ones. That is, the intermodulation noise level should be reduced by about three orders of magnitude. This high noise attenuation should even become more important if one chooses to modulate the phase of the Raman beam at the first optimum modulation frequency $f_\mathrm{m}^{(1)} = f_\mathrm{i}$ since in a continous mode of operation the modulation frequency is a free parameter. This general result highlights clearly the potential stability improvement in the measurement of the rotation rate that can be expected from a continuous operation.

In this paper, we have restricted our analysis to a single gyroscope with one atom source. Actually, cold atom gyroscopes are generally dual interferometers with two opposite atom sources designed to be operated in a differential mode to reject common mode noise. In principle,

our model can also be extended to take into account dual gyroscopes by making the analysis on the sum or the difference of the individual signal from each interferometer and by adapting the compensation scheme that cancels the inertial phase shift.

6 Conclusion

We have evaluated the behavior of aliasing noises that might appear in cold atom interferometers like gyroscopes. The model used to do this analysis takes into account a Mach-Zehnder interrogation and assumes the use of a servo-loop for the measurement of the rotation rate, making it a useful tool to investigate the performances associated to different modes of operation.

Theoretical results, valid for an idealized spatial-domain gyroscope with monokinetic atoms, show that in the case of a continuous mode of operation the overall intermodulation noise can be completely suppressed with a square wave phase modulation of the last Raman beam and a square demodulation for any modulation frequency. For a pulsed gyroscope, it is also possible to entirely suppress the aliasing noises, due to the Dick effect, if the launching frequency is equal to one of the optimum launching frequencies $f_{\mathrm{L}}^{(k)} = 2kf_{\mathrm{i}}$ where $f_{\mathrm{i}} = 1/2T$ is the interrogation frequency of the Mach-Zehnder interrogation.

For a real gyroscope with non-monokinetic atoms and a continuous mode of operation, the complete suppression of the intermodulation noises for any modulation frequency holds of course no more. But the Allan deviation of the residual overall intermodulation noise should remain well below the value corresponding to a pulsed operation for any modulation frequency. An estimate for typical parameters of a cold atom gyroscope yields a decrease of the Allan deviation of three orders of magnitude with respect to the value corresponding to a usual pulsed mode of operation. This very low residual aliasing noise level should even be further decreased if the modulation frequency is chosen equal to the first optimum modulation frequency $f_{\mathrm{L}}^{(1)} = f_{\mathrm{i}}$ showing clearly the potential stability improvement expected for a cold atom gyroscope operated in a continuous mode.

This work was supported by funding from the European Science Foundation within the EuroQUASAR program.

Appendix A: Fourier coefficients c_{2k}

For the calculation of the Fourier coefficients c_{2k} in (38), we consider that the modulation waveform $c(t)$ is an odd periodic function of time of frequency f_{m} with $|c(t)| \leq 1$. The demodulation function $d(t)$ is supposed to be a square waveform of frequency f_{m} with $|d(t)| = 1$ and also an odd function of time. Under these conditions, the spectrum of the deterministic function

$$a(t) = u(t - T_{\mathrm{det}})\, d(t - T_{\mathrm{d}}) \tag{A.1}$$

will contain only even harmonics of the modulation frequency f_{m} with the function $u(t)$ given by

$$u(t) = \sin\big(\phi_{\mathrm{m}}\, c(t)\big) \tag{A.2}$$

for a phase modulation of depth ϕ_{m} of the last Raman beam only. The complex coefficients c_{2k} of its Fourier series development can be calculated by

$$c_{2k} = \frac{2}{T_{\mathrm{m}}} \int_{-T_{\mathrm{m}}/4}^{T_{\mathrm{m}}/4} a(t)\, e^{-i4k\pi f_{\mathrm{m}} t}\, dt \tag{A.3}$$

where T_{m} is the modulation period. Let u_{2p+1} be the complex coefficients of the Fourier series development of the function $u(t)$ that contains only odd harmonics of the modulation frequency. Then, it comes

$$\begin{aligned} c_{2k} = -\frac{4}{\pi}\, e^{-i4k\pi f_{\mathrm{m}} T_{\mathrm{d}}} \sum_{p=0}^{+\infty} \frac{u_{2p+1}}{(2p+1)^2 - (2k)^2} \\ \times \Big\{ 2k\, \sin\big((2p+1)2\pi f_{\mathrm{m}}(T_{\mathrm{d}} - T_{\mathrm{det}})\big) \\ - i(2p+1) \cos\big((2p+1)2\pi f_{\mathrm{m}}(T_{\mathrm{d}} - T_{\mathrm{det}})\big) \Big\} \end{aligned} \tag{A.4}$$

where T_{d} and T_{det} are respectively the delay time of the demodulation waveform and the detection time. Usually, the demodulation of the output signal is performed in phase with the modulation waveform which means, for a monokinetic beam, that $T_{\mathrm{d}} = T_{\mathrm{det}}$ for $T_{\mathrm{det}} < T_{\mathrm{m}}$. Thus, we obtain finally for the Fourier coefficients c_{2k} the following result

$$c_{2k} = \frac{4i}{\pi}\, e^{-i4k\pi f_{\mathrm{m}} T_{\mathrm{det}}} \sum_{p=0}^{+\infty} \frac{(2p+1) u_{2p+1}}{(2p+1)^2 - (2k)^2}. \tag{A.5}$$

Let us examine in more details the particular case when the modulation waveform $c(t)$ is a square waveform with $|c(t)| = 1$. In that case, the coefficients u_{2p+1} are given by

$$u_{2p+1} = -\frac{2i}{\pi} \sin(\phi_{\mathrm{m}}) \frac{1}{2p+1} \tag{A.6}$$

and we get

$$c_{2k} = \frac{8}{\pi^2} \sin(\phi_{\mathrm{m}})\, e^{-i4k\pi f_{\mathrm{m}} T_{\mathrm{det}}} \sum_{p=0}^{+\infty} \frac{1}{(2p+1)^2 - (2k)^2}. \tag{A.7}$$

We can already note that the module $|c_{2k}|$ of these coefficients, which appears in the Allan variance (51), does not depend on the modulation frequency. Let us now show the particular property of the sum appearing in the above formula. By making use of the following relation [20]

$$\sum_{\substack{p=1 \\ p \neq m}}^{+\infty} \frac{1}{p^2 - m^2} = \frac{3}{4m^2} \tag{A.8}$$

where $m \geq 1$ is an integer, we can write

$$\sum_{\substack{p=1\\p\neq 2k}}^{+\infty} \frac{1}{p^2-(2k)^2} = \sum_{p=1}^{+\infty} \frac{1}{(2p+1)^2-(2k)^2} + \sum_{\substack{p=1\\p\neq k}}^{+\infty} \frac{1}{(2p)^2-(2k)^2} = \frac{3}{4(2k)^2}. \quad \text{(A.9)}$$

The last sum can be rewritten as

$$\sum_{\substack{p=1\\p\neq k}}^{+\infty} \frac{1}{(2p)^2-(2k)^2} = \frac{1}{4}\sum_{\substack{p=1\\p\neq k}}^{+\infty} \frac{1}{p^2-k^2} = \frac{1}{4}\,\frac{3}{4k^2} \quad \text{(A.10)}$$

and we can then deduce from (A.9) that

$$\sum_{p=1}^{+\infty} \frac{1}{(2p+1)^2-(2k)^2} = 0 \quad \text{(A.11)}$$

for any integer $k \geq 1$. The consequence is that all the Fourier coefficients $c_{2k} = 0$ for $k \geq 1$, except c_0 given by

$$c_0 = \frac{8}{\pi^2}\sin(\phi_{\rm m}) \sum_{p=0}^{+\infty} \frac{1}{(2p+1)^2} = \sin(\phi_{\rm m}) \quad \text{(A.12)}$$

which gives $c_0 = 1$ for the optimum phase modulation depth of $\phi_{\rm m} = \pi/2$. Note that this result is not surprising since, in the monokinetic case, the function $a(t)$ is the result of a product, in phase, of two perfect square waveforms of the same period and amplitude which gives a constant equals to one whatever the time is. Hence, all the Fourier coefficients $c_{2k} = 0$ and $c_0 = 1$. Moreover, this is true for any modulation frequency.

However, this property is only valid in the case of an ideal detector with unlimited bandwidth and for a square wave phase modulation of one Raman beam, and in particular of the last Raman beam as assumed here. In general, the cutoff frequency in the high of a real detector will introduce a deformation of the modulated output signal of the interferometer leading to non-vanishing Fourier coefficients c_{2k} since $a(t)$ will no longer be a product of two perfect square waveforms.

Other types of modulation waveforms or a modulation (inclusive a square wave phase modulation) of two or of the three Raman beams would result in Fourier coefficients c_{2k} that will depend on the modulation frequency even for a monokinetic beam and with a demodulation in phase. It means that these Fourier coefficients will always be different from zero except for specific modulation frequencies for which they will cancel.

Appendix B: Coefficients C_0, $C_{2k}^{\beta}(f)$ and $C_{2k}^{\rm M}(f)$

In the case of a real continuous non-monokinetic atomic beam, the coefficients C_0, $C_{2k}^{\beta}(f)$ for $\beta =$ RLO, L or CLO and $C_{2k}^{\rm M}(f)$, appearing in the Allan variance (67), are obtained by an averaging over the atomic velocity distribution $\rho(v)$ of the product of the Fourier coefficients (A.4) with the corresponding transfer functions. They are calculated by the following relations

$$\begin{aligned} C_0 &= \int_0^{+\infty} \rho(v)\,\frac{\bar{v}}{v}\,c_0(f_{\rm m},v)\,dv \\ C_{2k}^{\beta}(f) &= \int_0^{+\infty} \rho(v)\,c_{2k}^{*}(f_{\rm m},v)\,H_{\phi}^{\beta}(f,v)\,dv \\ C_{2k}^{\rm M}(f) &= \int_0^{+\infty} \rho(v)\,\frac{\bar{v}^2}{v^2}\,c_{2k}^{*}(f_{\rm m},v)\,H_{\phi}^{\rm M}(f,v)\,dv \end{aligned} \quad \text{(B.1)}$$

where $\bar{v}$ is the mean atomic velocity and the star denotes the complex conjugate. $c_0(f_{\rm m},v)$ and $c_{2k}(f_{\rm m},v)$ are the Fourier coefficients determined in Appendix A that depend now on the modulation frequency and the velocity. $H_{\phi}^{\beta}(f,v)$ and $H_{\phi}^{\rm M}(f,v)$ are the normalized and dimensionless transfer functions, defined in (32) and (36), in which the velocity dependence is obtained by replacing the constant transit time T and detection time $T_{\rm det}$ by their dependence on the atomic velocity $T(v) = Lv^{-1}$ and $T_{\rm det}(v) = L_{\rm det}v^{-1}$.

For the specific case of a square wave phase modulation with the optimum modulation depth and a demodulation of the output signal in phase with the modulation waveform, i.e. $T_{\rm d} = \overline{T}_{\rm det}$ for $\overline{T}_{\rm det} < T_{\rm m}$ with $\overline{T}_{\rm det} = L_{\rm det}\bar{v}^{-1}$ being the mean detection time, the Fourier coefficients are given from (A.4) by the expressions

$$c_0(f_{\rm m},v) = \frac{8}{\pi^2}\sum_{p=0}^{+\infty}\frac{1}{(2p+1)^2} \times\cos\left((2p+1)\,2\pi f_{\rm m}\,(\overline{T}_{\rm det} - L_{\rm det}v^{-1})\right) \quad \text{(B.2)}$$

and

$$c_{2k}(f_{\rm m},v) = \frac{8}{\pi^2}\sum_{p=0}^{+\infty}\frac{1}{(2p+1)^2-(2k)^2} \times\left\{\cos\left((2p+1)\,2\pi f_{\rm m}\,(\overline{T}_{\rm det} - L_{\rm det}v^{-1})\right) + i\,\frac{2k}{2p+1}\,\sin\left((2p+1)\,2\pi f_{\rm m}\,(\overline{T}_{\rm det} - L_{\rm det}v^{-1})\right)\right\} \quad \text{(B.3)}$$

with the constant phase term droped.

References

1. *Atom Interferometry*, edited by P.R. Berman (Academic Press, San Diego, 1997)
2. F. Riehle, T. Kister, A. Witte, J. Helmcke, C.J. Bordé, Phys. Rev. Lett. **67**, 177 (1991)

3. T.L. Gustavson, A. Landragin, M. Kasevich, Class. Quantum Grav. **17**, 2385 (2000)
4. T. Müller, M. Gilowski, M. Zaiser, P. Berg, Ch. Schubert, T. Wendrich, W. Ertmer, E.M. Rasel, Eur. Phys. J. D **53**, 273 (2009)
5. A. Gauguet, B. Canuel, T. Lévèque, W. Chaibi, A. Landragin, Phys. Rev. A **80**, (2009)
6. A. Peters, K.Y. Chung, S. Chu, Metrologia **38**, 25 (2001)
7. J. Le Gouët, T.E. Mehlstäubler, J. Kim, S. Merlet, A. Clairon, A. Landragin, F. Pereira Dos Santos, Appl. Phys. B **92**, 133 (2008)
8. A. Clairon, P. Laurent, G. Santarelli, S. Ghezali, S.N. Lea, M. Bahoura, IEEE Trans. Instrum. Meas. **44**, 128 (1995)
9. R. Wynands, S. Weyers, Metrologia **42**, 64 (2005)
10. G. Santarelli, C. Audoin, A. Makdissi, P. Laurent, G.J. Dick, A. Clairon, IEEE Trans. Ultrason. Ferroelec. Freq. Contr. **45**, 887 (1998)
11. G.J. Dick, in *Proc. 19th Precise Time and Time Interval meeting, Redendo Beach, CA, USA, 1987*, pp. 133–147
12. G.J. Dick, J.D. Prestage, C.A. Greenhall, L. Maleki, in *Proc. 22th Precise Time and Time Interval meeting, Vienna, VA, USA, 1990*, pp. 487–508
13. A. Luiten, A. Mann, M. Costa, D. Blair, IEEE Trans. Instrum. Meas. **44**, 132 (1995)
14. K.A. Moler, D.S. Weiss, M. Kasevich, S. Chu, Phys. Rev. A Gen. Phys. **45**, 342 (1992)
15. A. Papoulis, *Probability, Random Variables, and Stochastic Processes* (McGraw-Hill, New York, 1984)
16. W.B. Davenport Jr., W.L. Root, *An Introduction to the Theory of Random Signals and Noise* (IEEE Press, New York, 1987), Chap. 4
17. P. Cheinet, B. Canuel, F. Pereira Dos Santos, A. Gauguet, F. Yver-Leduc, A. Landragin, IEEE Trans. Instrum. Meas. **57**, 1141 (2008)
18. A. Makdissi, E. de Clercq, C. Audoin, A. Clairon, in *Proc. 1997 IEEE Int. Freq. Contr. Symp. Orlando, FL, USA* (1998), pp. 263–269
19. A. Makdissi, *Traitement de Signal Appliqué aux Etalons Primaires de Fréquence: Amélioration de leur Exactitude et de leur Stabilité*, Ph.D. thesis, University of Paris-Sud, 1999
20. I.S. Gradshteyn, I.M. Ryzhik, *Table of Integrals, Series, and Products* (Academic Press, New York, 1980)